1
Basic Principles

1.1
Atomic structure

The basic processes in optical atomic spectrometry involve the outer electrons of the atomic species and therefore its possibilities and limitations can be well understood from the theory of atomic structure itself. On the other hand, the availability of optical spectra was decisive in the development of the theory of atomic structure and even for the discovery of a series of elements. With the study of the relationship between the wavelengths of the chemical elements in the mid-19th century a foundation was obtained for the relationship between the atomic structure and the optical line emission spectra of the elements.

In 1885 Balmer published that for a series of atomic lines of hydrogen a relationship between the wavelengths could be found and described as:

$$\lambda = k \cdot n^2/(n^2 - 4) \tag{1}$$

where $n = 2, 3, 4, \ldots$ for the lines H_α, H_β, H_γ etc.

Eq. (1) can also be written in wavenumbers as:

$$\nu' = 1/\lambda = R(1/2^2 - 1/n^2) \tag{2}$$

where ν' is the wavenumber (in cm^{-1}) and R is the Rydberg constant (109 677 cm^{-1}). The wavenumbers of all so-called series in the spectrum of hydrogen are given by:

$$\nu' = 1/\lambda = R(1/n_1^2 - 1/n_2^2) \tag{3}$$

where n_2 is a series of numbers $> n_1$ and with $n_1 = 1, 2, 3, 4, \ldots$ for the Lyman, Balmer, Paschen, and Pfund series, respectively.

Rydberg applied the formula of Balmer as:

$$\nu' = R \cdot Z^2(1/n_1^2 - n_2^2) \tag{4}$$

Analytical Atomic Spectrometry with Flames and Plasmas. José A. C. Broekaert

ISBN: 3-527-31282-X

where Z is the effective charge of the atomic nucleus. This formula then also allows calculation of the wavelengths for other elements. The wavenumbers of the atomic spectral lines can thus be calculated from the difference between two positive numbers, called terms, and the spectrum of an element accordingly contains a large number of spectral lines each of which is related by two spectral terms.

The significance of the spectral terms had already been reflected by Bohr's theory, where it is stated that the atom has a number of discrete energy levels related to the orbits of the electrons. These energy levels are the spectral terms. As long as an electron is in a defined orbit no electromagnetic energy is emitted but when a change in orbit occurs, another energy level is reached and the excess energy is emitted in the form of electromagnetic radiation. The wavelength is given according to Planck's law as:

$$E = h \cdot \nu = h \cdot c/\lambda \tag{5}$$

Here $h = 6.623 \times 10^{-27}$ erg s, ν is the frequency in s^{-1}, $c = 3 \times 10^{10}$ cm/s is the velocity of light, and λ is the wavelength in cm.

Accordingly:

$$\begin{aligned} \nu' &= 1/\lambda = E/h \cdot c = E_1/(h \cdot c) - E_2/(h \cdot c) \\ &= T_1 - T_2 \end{aligned} \tag{6}$$

T_1 and T_2 are the Bohr energy levels and the complexity of the emission spectra can be related to the complexity of the structure of the atomic energy levels.

For an atom with a nucleus charge Z and one valence electron, the energy of this electron is given by:

$$E = -\frac{2 \cdot \pi \cdot Z^2 \cdot e^4 \cdot \mu}{n^2 h^2} \tag{7}$$

$\mu = m \cdot M/(m + M)$, with m being the mass of the electron and M the mass of the nucleus; n is the main quantum number $(n = 1, 2, 3, \ldots)$ and gives the order of the energy levels. Through the movement around the atomic nucleus, the electron has an orbital impulse moment L of which the absolute value is quantitized as:

$$|L| = h/(2\pi)\sqrt{l(l+1)} \tag{8}$$

l is the orbital quantum number and has values of: $0, 1, \ldots, (n-1)$.

The elliptical orbits can take on different orientations with respect to an external electric or magnetic field and the projections on the direction of the field also are quantized and given by:

$$L_z = h/(2\pi)m_l \tag{9}$$

L_z is the component of the orbital momentum along the field axis for a certain angle, $m_l = \pm l, \pm(l-1), \ldots, 0$ is the magnetic quantum number and for each value of l it may have $(2l+1)$ values.

When a spectral line source is brought into a magnetic field, the spectral lines start to display hyperfine structures, which is known as the Zeeman effect. In order to explain these hyperfine structures it is accepted that the electron rotates around its axis and has a spin momentum S for which:

$$|S| = h/(2\pi)\sqrt{S(S+1)} \tag{10}$$

The spin quantum number m_s determines the angles possible between the axis of rotation and the external field as:

$$s_z = h/(2\pi)m_s \tag{11}$$

where $m_s = \pm\frac{1}{2}$.

The orbital impulse momentum and the spin momentum are vectors and determine the total impulse momentum of the electron J as:

$$J = L + S \quad \text{with } |J| = h/(2\pi)\sqrt{j(j+1)} \tag{12}$$

$j = l \pm s$ and is the total quantum number.

In the case of an external magnetic or electrical field, the total impulse momentum also has a component along the field, whose projections on the field are quantized and given by:

$$J_z = h/(2\pi) \times m_j \quad \text{with } m_j = \pm j, \pm(j-1), \ldots, 0 \tag{13}$$

This corresponds with a possible $2j+1$ orientations.

The atomic terms differ by their electron energies and can be characterized by the quantum numbers using the so-called term symbols:

$$n^m l_j \tag{14}$$

Here $l = 0, 1, 2, \ldots$ and the corresponding terms are given the symbols s (sharp), p (principal), d (diffuse), f (fundamental), etc., originally relating to the nature of different types of spectral lines: n is the main quantum number, m is the multiplicity ($m = 2s \pm 1$), and j is the total internal quantum number. The energy levels of each element can be given in a term scheme. In such a term scheme, also indicated are which transitions between energy levels are allowed and which ones are forbidden. This is reflected by the selection rules. According to these, only those transitions are allowed for which Δn has an integer value and at the same time $\Delta l = \pm 1$, $\Delta j = 0$ or ± 1 and $\Delta s = 0$. The terms of an atom with one valence electron can easily be found, e.g., for Na ($1s^2 2s^2 2p^6 3s^1$), in the ground level: $3^2S_{1/2}$ [$l = 0$ (s), $m = 2.1/2 + 1 = 2$ as $s = 1/2$ and $j = 1/2$ ($j = |l \pm s|$)]. When the 3s electron

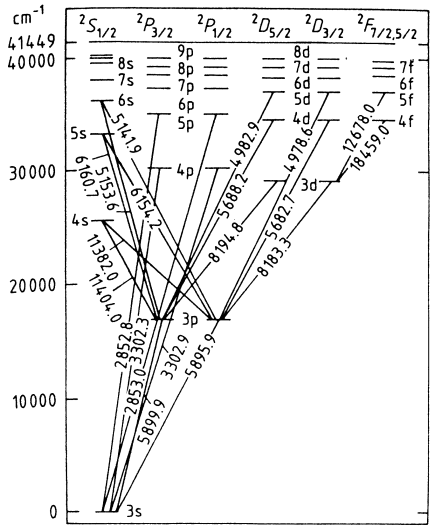

Fig. 1. Atomic energy level diagram for the sodium atom. (Reprinted with permission from Ref. [3].)

goes to the 3p level, the term symbol for the excited level is: $3^2P_{1/2,3/2}$ [$l = 1$ (p), $m = 2.1/2 + 1 = 2$ as $s = 1/2$ and $j = 1/2, 3/2$]. The terms have a multiplicity of 2 and accordingly the lines have a doublet structure.

The term schemes of the elements are well documented in the work of Grotrian [3]. For the case of the Na atom the term scheme is represented in Fig. 1.

When atoms have more than one valence electron, the term schemes become more complex as a coupling between the impulse and orbital momenta of the individual electrons occurs. According to Russell and Saunders ($L - S$) a coupling applies, where the orbital moments of all electrons have to be coupled to a total orbital momentum, as with the spin momentum. This coupling applies for elements with Z below 20, where it is accepted that the spin–orbital interactions are much lower than the spin–spin and the orbital–orbital interactions. The fact that none of the electrons in an atom can have the same set of quantum numbers is known as the Pauli rule. The total quantum number L is obtained as $L = \Sigma l$, $S = \Sigma s$ and $J = L - S, \ldots, L + S$. The term symbol accordingly becomes:

$$^{m}L_J \tag{15}$$

For the case of magnesium ($1s^2 2s^2 2p^6 3s^2$), the ground level is 3^1S_0 (as there are two 3s electrons which must have antiparallel spins $L = 0$ as $l_1 = 0$ and $l_2 = 0$, $S = 0$ as $s_1 = 1/2$ and $s_2 = -1/2$, and $J = 0$ as both L and $S = 0$). The excited level ($1s^2 2s^2 2p^6 3s3p$) is characterized by the terms: 3^1P_1 ($L = 1$ as $l_1 = 0$ and $l_2 = 1$, $S = 0$ as $s_1 = 1/2$ and $s_2 = -1/2$, and $J = |L \pm 1| = 1$) but also 3^3P_2, 3^3P_1 and 3^3P_0 (as for the spins $s_1 = 1/2$ and $s_2 = 1/2$, $S = 1$, and further $J = 0, 1, 2$ parallel). Here, singlet ($m = 1$) and triplet ($m = 3$) terms are present in the term scheme. Also a jj coupling is possible, when the interaction between spin and orbital momentum of the individual electrons is decisive.

With a number of electrons the coupling becomes more complex and leads to a high number of terms and accordingly line-rich atomic spectra. Moreover, not only neutral atoms but also ions with different levels of ionization have term schemes, making the optical spectra very line rich. Indeed, for 90 elements between 200 and 400 nm more than 200 000 atomic lines have been listed, and many others are missing from the tables.

From Planck's law, as given by Eq. (5), the relationship between the optical atomic spectra of the elements and energy level transitions of the valence electrons can be understood. Indeed, the wavelength corresponding to a transition over an energy difference of 1 eV according to Planck's law corresponds to a wavelength of: $1\ \text{eV} = 1.6 \times 10^{-12}\ \text{erg} = 6.62 \times 10^{-27}\ \text{erg s} \times 3 \times 10^{10}\ \text{cm/s} \times 1/\lambda\ \ (\text{cm})$ or 1240 nm. Accordingly, the optical wavelength range of 200–800 nm corresponds to energies of 2–7 eV, this being the range involved in transitions of the valence electrons.

1.2 Plasmas

Partially ionized gases are usually denoted as plasmas [4]. They contain molecules, radicals, and atoms but also ions and free electrons and result from the coupling of energy with matter in the gaseous state. As has been previously stated for atoms, the radicals, molecules, and ions also present in the plasma can be in their ground states or in excited states and radiation can be emitted or absorbed when transitions from one state to another occur. The wavelength of the radiation can be obtained from Planck's law whereas the intensities of the discrete lines depend on the number densities of the species and the states involved.

Transfer of energy for the different species in a plasma results from the non-radiative as well as from the radiative processes taking place. Non-radiative processes involve collisions and radiative processes involve emission, absorption, and fluorescence of radiation. The efficiency of collision processes is described by the cross section $\sigma(v)$. This reflects the loss in impulse that a particle with mass m and velocity v undergoes when it collides with a particle with mass M. It can be given by:

$$\sigma(v) = 2\pi \int_0^{\pi} p(v,\theta)(1 - \cos\theta)\sin\theta\,\mathrm{d}\theta \tag{16}$$

This expression shows that apart from loss of momentum a change in direction may also result from collisions. The mean collision cross section is denoted as: $\langle\sigma(v)\rangle$. A collision frequency is described as $\langle\sigma(v)\cdot v\rangle$ and a mean collision frequency as $\langle\sigma(v)\cdot v\rangle/\langle v\rangle$.

Apart from the cross section, however, the velocity distribution for a given species is important for describing the energy transfer in a plasma.

In the case of a Maxwell distribution the velocity distribution is given by:

$$\mathrm{d}n/n = 2/(\sqrt{\pi}) \cdot \sqrt{u'} \cdot \mathrm{e}^{-u'} \cdot \mathrm{d}u' \tag{17}$$

In the case of a so-called Druyvenstein distribution:

$$\mathrm{d}n/n = 1.039 \cdot \sqrt{u'} \cdot \exp(-0.548 \cdot u'^2)\,\mathrm{d}u' \tag{18}$$

$u' = E/kT$, where E is the mean energy of the particles and T is the absolute temperature.

For a plasma contained in a closed system and which is in so-called thermal equilibrium, the population of the excited levels for every type of particle is given by Boltzmann's law:

$$n_q/n_0 = g_q/g_0 \cdot \exp(-E_q/kT) \tag{19}$$

n_q is the number density of particles in the excited state, n_0 is the number density of particles in the ground state, g_q and g_0 are the statistical weights of the corresponding levels, E_q is the excitation energy of the state q, k is Boltzmann's constant (1.38×10^{-16} erg K), and T is the absolute temperature. In Eq. (19) a relationship is formulated between the temperature and the atom number densities in a single excited state and in the ground state, respectively. As the latter is not constant, the Boltzmann equation can be better formulated as a function of the total number of particles n distributed over all states. Then

$$n_q/n = [g_q \cdot \exp(-E_q/kT)]/[\Sigma_\mathrm{m} g_\mathrm{m} \cdot \exp(-E_\mathrm{m}/kT)] \tag{20}$$

as $n = \Sigma_\mathrm{m} n_\mathrm{m}$. The sum $Z_\mathrm{m} = \Sigma_\mathrm{m} g_\mathrm{m} \cdot \exp(-E_\mathrm{m}/kT)$ is the partition function. This is a function of the temperature and the coefficients of this function for a large number of neutral and ionized species are listed in the literature (see, e.g., Ref. [5]). When E_q is expressed in eV, Eq. (20) can be written as:

$$\log n_{aq} = \log n_a + \log n_q - (5040)/T \cdot V_q - \log Z \tag{21}$$

1.3 Emission and absorption of radiation

In a steady-state plasma the number of particles leaving an energy level per unit of time equals the number returning to this level [6]. In order to characterize such an equilibrium, all processes which can lead to excitation as well as to de-excitation have to be considered. The most important energy exchange processes in a plasma are as follows.

- (1a) Collisions in which atoms are excited to a higher level by collision with energetic neutrals (collisions of the first kind).
- (1b) Collisions in which excited neutrals lose energy without emission of radiation (collisions of the second kind).
- (2a) Excitation by collision with electrons.
- (2b) De-excitation where energy is transferred to electrons.
- (3a) Excitation of atoms by the absorption of radiation.
- (3b) De-excitation of atoms by spontaneous or stimulated emission.

When n is the number density of the first type of particles and N is that of a second species that is present in excess ($n \ll N$), the following equilibria can be considered:

$$\alpha \cdot N \cdot n_0 = \beta \cdot N \cdot n_q \tag{22}$$

$$\alpha_e \cdot n_e \cdot n_0 = \beta_e \cdot n_e \cdot n_q \tag{23}$$

$$B' \cdot \rho_\nu \cdot n_0 = (A + B \cdot \rho_\nu) \cdot n_q \tag{24}$$

n_e is the electron number density, A, B, and B' are the Einstein transition probabilities for spontaneous emission, stimulated emission and absorption and α_e, α, β_e and β are functions of the cross sections for the respective processes as well as of the velocity distribution of the particles involved. ρ_ν is the radiation density (frequency ν).

When the system is in so-called thermodynamic equilibrium, the neutrals and the electrons have the same Maxwell velocity distribution and at a temperature T we have:

$$n_q/n_0 = \alpha/\beta = \alpha_e/\beta_e = B'/(A/\rho_\nu + B) = g_q/g_0 \cdot \exp(-E_q/kT) \tag{25}$$

Thus, each process is in equilibrium with the inverse process and the Boltzmann distribution of each state is maintained by collisions of the first and the second kind, including those with electrons, and there are no losses of energy through the emission of radiation or any absorption of radiation from an external source.

In a real radiation source this perfect equilibrium cannot exist and there are losses of energy as a result of the emission and absorption of radiation, which also have to be considered. However, as long as both only slightly affect the energy balance, the system is in so-called local thermal equilibrium and:

$$\begin{aligned} &\alpha \cdot N \cdot n_0 + \alpha_e \cdot n_e \cdot n_0 + B' \cdot \rho_\nu \cdot n_0 \\ &\quad = \beta \cdot N \cdot n_q + \beta_e \cdot n_e \cdot n_q + (A + B \cdot \rho_\nu) \cdot n_q \end{aligned} \tag{26}$$

from which n_q/n_0 can be calculated as:

$$n_q/n_0 = (\alpha \cdot N + \alpha_e \cdot n_e + B' \cdot \rho_\nu)/[\beta \cdot N + \beta_e \cdot n_e + (A + B \cdot \rho_\nu)] \tag{27}$$

The population of the excited states is determined by the excitation processes in the radiation source, as reflected by the coefficients in Eq. (26).

In the case of a DC arc for instance $\alpha \cdot N \gg \alpha_e \cdot n_e + B' \cdot \rho_\nu$ and $\beta \cdot N \gg \beta_e \cdot n_e + (A + B \cdot \rho_\nu)$. This leads to:

$$n_q/n_0 = \alpha/\beta = g_q/g_0 \cdot \exp(-E_q/kT) \tag{28}$$

As the radiation density is low, it can be accepted that the DC arc plasma is in thermal equilibrium. The excited states are produced predominantly and decay through collisions with neutrals.

The simplification which leads to Eq. (28) does not apply to discharges under reduced pressure, where collisions with electrons are very important as are the radiation processes. Moreover, the velocity distributions are described by the Druyvenstein equation. These sources are not in thermal equilibrium.

Excited states are prone to decay because of their high energy and therefore mainly have short lifetimes. The decay can occur by collisions with surrounding particles (molecules, atoms, electrons or ions) or by emission of electromagnetic radiation. In the latter case, the wavelength is given by Planck's law. When the levels q and p are involved, the number of spontaneous transitions per unit of time is given by:

$$-\mathrm{d}N_q/\mathrm{d}t = A_{qp} \cdot N_q \tag{29}$$

where A_{qp} is the Einstein coefficient for spontaneous emission (in s^{-1}). When considering an optically thin system with atoms in the excited state q, which decay spontaneously to a level p under the emission of radiation, the number of transitions per unit time at each moment is proportional to the number of atoms in the state q. When several transitions can start from level q ($q \to p_1, q \to p_2, \ldots, q \to p_n$) Eq. (29) becomes:

$$-\mathrm{d}N_q/\mathrm{d}t = N_q \cdot \Sigma_p A_{qp} = N_q \cdot \nu_q \tag{30}$$

Here, ν_q is the inverse value of the mean lifetime of the excited state q. For levels from which a decay by an allowed radiative transition can take place, the lifetime is of the order of 10^{-8} s. When no radiative transitions are allowed we have metastable levels (e.g. Ar 11.5 and 11.7 eV), which can only decay through collisions. Therefore, such levels in the case of low-pressure discharges may have very long lifetimes (up to 10^{-1} s).

In the case of the absorption of electromagnetic radiation with a frequency ν_{qp} and a radiation density ρ_ν, the number density of N_q increases as:

$$\mathrm{d}N_q/\mathrm{d}t = B_{qp} \cdot N_q \cdot \nu_\rho \tag{31}$$

For the case of stimulated emission, atoms in the excited state q only decay when they receive radiation of the wavelength λ_{qp} and

$$-\mathrm{d}N_q\,\mathrm{d}t = B_{qp} \cdot N_q \cdot \rho_\nu \tag{32}$$

For the case of thermal equilibrium:

$$g_q \cdot B_{qp} = g_p \cdot B_{pq} \tag{33}$$

and:

$$A = (8\pi h\nu^3/c^3) \times B_{qp} = (8\pi h\nu^3/c^3) \times (g_q/g_p) \times B_{qp} \tag{34}$$

where g_p and g_q are the degeneratives of the respective levels with $g = 2J + 1$.

The intensity (I_{qp}) of an emitted spectral line is proportional to the number density of atoms in the state q:

$$I_{qp} = A_{qp} \cdot n_{aq} \cdot h \cdot \nu_{qp} \tag{35}$$

or after substitution of n_{aq}, or n_q for atomic species, according to Eq. (20):

$$I_{qp} = A_{qp} \cdot h \cdot \nu_{qp} \cdot n_\mathrm{a} \cdot (g_q/Z_\mathrm{a}) \cdot \exp(-E_q/kT) \tag{36}$$

When multiplying with $d/(4\pi)$, where d is the depth of the source (in cm), one obtains the absolute intensity. T is the excitation temperature, which can be determined from the intensity ratio for two lines (a and b) of the same ionization stage of an element as:

$$T = [5040(V_\mathrm{a} - V_\mathrm{b})]/\{\log[(gA)_\mathrm{a}/(gA)_\mathrm{b}] - \log(\lambda_\mathrm{a}/\lambda_\mathrm{b}) - \log(I_\mathrm{a}/I_\mathrm{b})\} \tag{37}$$

In order to determine the excitation temperature with a high precision, the thermometric species should have a high degree of ionization, otherwise the temperature or the geometry of the discharge will change when the substance is brought into the source. Furthermore, the difference between V_a and V_b must be large. Indeed, the error of the determination can be obtained by differentiating Eq. (37):

$$\mathrm{d}T/T = T/[5040(V_\mathrm{a} - V_\mathrm{b})] \times 0.434 \times \mathrm{d}I/I \tag{38}$$

$(gA)_\mathrm{a}/(gA)_\mathrm{b}$ must be large when $(V_\mathrm{a} - V_\mathrm{b})$ is large and $I_\mathrm{a}/I_\mathrm{b}$ should not be particularly small or large. In addition, the transition probabilities must be accurately known. Indeed, the error of the determination of the temperature strongly depends on the accuracy of $(gA)_\mathrm{a}/(gA)_\mathrm{b}$, as by differentiating Eq. (37) with respect to $\log[(gA)_\mathrm{a}/(gA)_\mathrm{b}]$ one obtains:

$$\mathrm{d}T = T^2/[5040(V_\mathrm{a} - V_\mathrm{b})] \times \mathrm{d}[(gA)_\mathrm{a}/(gA)_\mathrm{b}] \tag{39}$$

Often the line pair Zn 307.206/Zn 307.59 is used, for which: $V_\mathrm{a} = 8.08$ eV and $V_\mathrm{b} = 4.01$ eV and $(gA)_\mathrm{a}/(gA)_\mathrm{b} = 380$ and:

$$T = 20510/[2.58 + \log[I_{307.6\ \mathrm{nm}}/I_{307.2\ \mathrm{nm}}]] \tag{40}$$

This line pair is very suitable because the ionization of zinc is low as a result of its relatively high ionization energy, the wavelengths are close to each other, which minimizes errors introduced by changes in the spectral response of the detector, and the ratio of the gA values is well known.

The excitation temperature can also be determined from the slope of the plot $\ln[I_{qp}/(g_q \cdot A_{qp} \cdot \nu_{qp})]$ or $\ln[I_{qp} \cdot \lambda/(gA_{qp})]$ versus E_q, which is $-1/k \cdot T$ as:

$$\ln[I_{qp}/(g_q \cdot A_{qp} \cdot \nu_{qp})] = \ln(h \cdot n/Z) - E_q/(k \cdot T) \tag{41}$$

The λ/gA values for a large number of elements (such as argon, helium, iron) and their lines have been compiled [6]. The determination of excitation temperatures in spatially inhomogeneous plasmas has been treated extensively by Boumans [7] and is described later (see Ref. [8]).

• Example
For the case of a 2 kW inductively coupled plasma the four iron lines Fe I 381.58 nm, Fe I 383.04 nm, Fe I 382.44 nm, and Fe I 382.58 nm have relative intensities of 5, 10, 2.3, and 7.4 a.u., respectively. When using the transition probability products gA of 66, 36, 1.26, and 26 (see Ref. [9]) as well as the excitation energies of 38175, 33096, 26140, and 33507 cm^{-1}, respectively, it can be calculated that the excitation temperature should be 5000 K.

Limitations to the spectroscopic measurement of the temperatures from line intensities lie in possible deviations from ideal thermodynamic behavior in real radiation sources, and also in the poor accuracy of transition probabilities. They can be calculated from quantum mechanics, and have been determined and compiled by Corliss and Bozman at NIST [10] from measurements using a copper DC arc. These tables contain line energy levels, transition probabilities, and the so-called oscillator strengths for ca. 25 000 lines between 200 and 900 nm for 112 spectra of 70 elements. Between the oscillator strengths f_{qp} (being 0.01–0.1 for non-resonance and nearer to 1 for resonance lines) and the transition probabilities there is the relationship [11]:

$$f_{qp} = (g_q/g_p) \times A_{qp} \times [(m \cdot c^3)/(8 \cdot \pi^2 \cdot e^2 \cdot \nu^2)] \tag{42}$$

and

$$f_{qp} = 1.499 \times 10^{-16} \times \lambda^2 \times g_q/g_p \times A_{qp} \tag{43}$$

As g is known to be $2J + 1$, oscillator strengths can be converted into transition probabilities and vice versa.

According to the classical dispersion theory, the relationship between the absorption and the number density of the absorbing atoms is given by:

$$\int K_\nu \cdot \mathrm{d}\nu = (\pi e^2)/mc \cdot N_\nu \cdot f \tag{44}$$

K_ν is the absorption coefficient at a frequency ν, m is the mass and e the charge of the electron, c is the velocity of light, N_ν is the density of atoms with a line at a frequency between ν and $\nu + \mathrm{d}\nu$ and is almost equal to N; f is the oscillator strength. This relationship applies purely to monochromatic radiation. As the widths of the absorption lines in most atom reservoirs are of the order 1–5 pm, the use of a primary source which emits very narrow lines would be advantageous. Indeed, when using a continuous source one would need a spectral apparatus with a practical resolving power of at least 500 000 to reach the theoretically achievable values of K_ν and this certainly would lead to detector noise limitations as a result of the low irradiances. Therefore, it is more advantageous to use sources which emit relatively few narrow lines and to use a low-resolution monochromator which just isolates the spectral lines in the spectra.

The relationship between the absorption A and the concentration of the absorbing atoms in an atom reservoir is given by the Lambert–Beer law. When I_0 is the intensity of the incident radiation, l is the length of the atom reservoir, and I is the intensity of the exiting radiation, the change in intensity $\mathrm{d}I$ resulting from the absorption within the absorption path length $\mathrm{d}l$ is given by:

$$-\mathrm{d}I = k \cdot I_0 \cdot c \cdot \mathrm{d}I \tag{45}$$

or

$$\int_{I_0}^{I} (\mathrm{d}I)/I = k \cdot c \cdot \int_0^l \mathrm{d}l \tag{46}$$

$A = \log(I_0/I) = \log(1/T)$, in which A is the absorbance and T the transmission. Accordingly, Eq. (46) becomes:

$$A = k \cdot c \cdot l \tag{47}$$

The absorbances are additive. The Lambert–Beer law, however, is only valid within a restricted concentration range. This is due to the fact that not all radiation reaching the detector has been absorbed to the same extent by the analyte atoms. Normally the calibration curve at high concentrations levels off asymptotically to the signal for the non-absorbed radiation. The latter consists of contributions from non-absorbed lines of the cathode material in the hollow cathode lamp or of lines of the filler gas within the spectral bandwidth of the monochromator. The calibration curve is only linear in the concentration range where the ratio of the widths of the emission to the absorption line is $<1/5$. Also, incomplete dissociation of analyte molecules leads to a curvature towards the concentration axis, and this incomplete dissociation then becomes limiting at high concentrations. A decrease in the ionization at higher analyte concentrations, however, may cause curvature away from the concentration axis. For all these reasons, in atomic absorption spectrometric measurements, deviations from linearity are common and the linear dynamic range is much smaller than in atomic emission or atomic fluorescence.

Line broadening

Atomic spectral lines have a physical width as a result of several broadening mechanisms [12].

The natural width of a spectral line is due to the finite lifetime of an excited state (τ). The corresponding halfwidth in terms of the frequency is given by:

$$\Delta\nu_{\mathrm{N}} = 1/(2\pi\tau) \tag{48}$$

For lines corresponding to transitions that are allowed according to the selection rules, lifetimes are of the order of 10^{-8} s and, accordingly, for most spectral lines this results in a natural broadening with a halfwidth of the order of 10^{-2} pm.

The Doppler spectral width results from the movement of the emitting atoms and their velocity component in the viewing direction. The respective halfwidth is given by:

$$\Delta\nu_{\mathrm{D}} = [2 \cdot \sqrt{(\ln 2)}/c] \cdot \nu_0 \cdot \sqrt{[(2 \cdot R \cdot T)/M]} \tag{49}$$

where c is the velocity of light, ν_0 is the frequency of the line maximum, R is the gas constant, and M is the atomic mass. The Doppler broadening thus strongly depends on the temperature. Accordingly, it is also often denoted as temperature broadening and reflects the kinetic energy of the radiating species (atoms, ions or molecules). The relevant temperature is denoted as the gas temperature or Doppler temperature. The measurement of the Doppler broadening thus allows the determination of the gas temperatures in spectroscopic sources (see line profiles in Fig. 2). For the light elements, the Doppler broadening is larger than it is for analytical lines with shorter wavelengths. For the Ca 422.6 nm line in the case of a hollow cathode discharge at a few mbar pressure, the Doppler broadening at 300 K for instance is 0.8 pm whereas at 2000 K it is 2 pm [13].

The Lorentzian broadening or pressure broadening results from the interaction between the emitting atoms of the element considered and atoms of other elements. The halfwidth is given by:

$$\Delta\nu_{\mathrm{L}} = (2/\pi) \cdot \sigma_{\mathrm{L}}^2 \cdot N\sqrt{[2 \cdot \pi \cdot R \cdot T \cdot (1/M_1 + 1/M_2)]} \tag{50}$$

M_1 and M_2 are the atomic masses, N is the concentration of the foreign atoms, and σ_{L} is their cross section. The pressure broadening is low in the case of discharges under reduced pressure. For the case of the Ca 422.6 nm line this type of broadening at a temperature of 300 K and a pressure of 9 mbar is only 0.02 pm. At atmospheric pressure, however, this type of line broadening is the predominant one.

Furthermore, isotopic structure and hyperfine structure, and also resonance broadening, resulting from the interaction between radiating and non-radiating atoms of the same species, and Stark broadening, resulting from interaction with electrical fields, contribute to the physical widths of the spectral lines.

The natural broadening and the Lorentzian broadening have a Lorentzian distribution, which is given by:

$$I(\nu) = I_0/\{1 + [2(\nu - \nu_0)/\Delta\nu]^2\} \tag{51}$$

The Doppler broadening has a Gaussian distribution, described by:

$$I(\nu) = I_0 \cdot \exp - \{[2(\nu - \nu_0)/2\Delta\nu_D] \cdot \sqrt{(\ln 2)}\} \tag{52}$$

The combination of both types of profile functions (which is normally due to the predominance of both pressure and temperature broadening) results in a so-called Voigt profile, which can be described by:

$$V(\alpha, \omega) = \alpha/\pi \int_{-\infty}^{+\infty} \{[\exp(-y^2 \cdot dy)]/[\alpha^2 + (\omega - y)]^2\} \tag{53}$$

$$\omega = 2(\nu - \nu_0)/\Delta\nu_D \cdot \sqrt{(\ln 2)} \quad \text{and} \quad \alpha = \Delta\nu_D \cdot \sqrt{(\ln 2)}$$

when the contribution of the natural width is neglected. From the physical line widths of the spectral lines, which in most cases are between 1 and 20 pm, and the information on the profile functions discussed above, the contributions of the different processes can be calculated by deconvolution methods. However, the experimentally measured full-widths at half maximum (FWHM) must be corrected for the bandwidth of the spectral apparatus used. In the determination of absorption profiles with the aid of very narrow bandwidth tunable laser sources, the spectral bandwidth of the probing beam can often be neglected. Equation (53), for example, can be solved by a mathematical progression as:

$$\begin{aligned} V(\alpha, \omega) = {} & \alpha/[\text{constant} \times (\alpha^2 + \omega^2)]\{1 + [3(\alpha^2 - \omega^2)/2(\alpha^2 + \omega^2)^2] \\ & + [3(\alpha^4 + 10\alpha^2\omega^2 + 5\omega^4)/4(\alpha^2 + \omega^2)^4] + \cdots\} \end{aligned} \tag{54}$$

From this solution α and ω and accordingly $\Delta\nu_L$ and $\Delta\nu_D$ can be determined, and from the latter the gas kinetic temperature. This is a measure of the kinetic energy of atoms and ions in the plasma.

Owing to the line broadening mechanisms, the physical widths of spectral lines in most radiation sources used in optical atomic spectrometry are between 1 and 20 pm. This applies both for atomic emission and atomic absorption line profiles. In reality, the spectral bandwidth of dispersive spectrometers is much larger than the physical widths of the atomic spectral lines.

The profiles of spectral lines as are obtained in plasma sources at atmospheric pressure are illustrated by the high-resolution records of a number of rare earth spectral lines obtained in the case of an inductively coupled plasma source (ICP) (Fig. 2) [14].

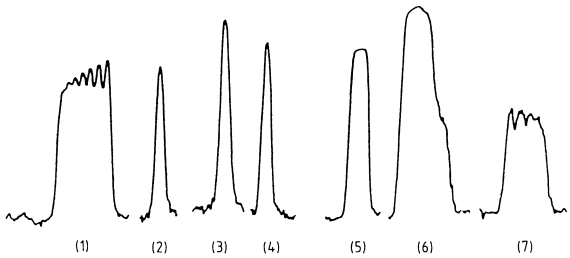

Fig. 2. Line profiles of some rare earth element atomic emission lines in inductively coupled plasma atomic emission spectrometry (photographic measurements obtained with a high-resolution grating spectrograph): theoretical resolving power: 460 000. (1): Ho II 345.6 nm, (2): Er II 369.2 nm, (3): Yb II 369.4 nm, (4): Y II 371.0 nm, (5): Tm II 376.1 nm, (6): Eu II 381.9 nm, and (7): La II 398.8 nm. (Reprinted with permission from Ref. [14].)

Self-absorption

The radiation emitted in a radiation source is absorbed by ground-state atoms of the same species. This phenomenon is known as self-absorption (for an explanation, see e.g., Ref. [15]). As the chance that an absorbed photon is re-emitted is <1, this causes the observed radiation to be weaker than the emitted radiation. When I_0 is the intensity emitted at the wavelength of the line maximum and $P_E(\nu)$ is the profile function, the intensity distribution for a line emitted by a radiation source over the profile of a line equals $I_0 \cdot P_E(\nu)$ and the intensity observed after the radiation has passed through a layer with a number density of absorbing atoms of n_A is:

$$I(\nu) = I_0 \cdot P_E(\nu) \cdot \exp[-\rho \cdot P_A(\nu)/P_A(\nu_0)] \tag{55}$$

ν_0 is the frequency at the line center, $P_A(\nu)$ is the absorption profile function, $P_A(\nu_0)$ is its value at the line center, and p is an absorption parameter:

$$p \approx B \cdot P_A(\nu) \cdot n_A \tag{56}$$

p increases with the absorption transition probability and thus is larger for resonance lines which stem from transitions ending at the ground level. It is also larger in sources with a high analyte number density n_A. As the absorption is maximal in the center of the line, self-absorption always leads to flatter line profiles. Self-absorption increases with the analyte number densities in the source, and with the number densities of emitting and absorbing analyte atoms the intensity of a line tends to that given by Planck's law for black-body radiation. When a minimum occurs in the absorption profile, then the line undergoes so-called self-reversal, and the absorption parameter is then >1. Self-reversal only occurs when there is a strong temperature gradient in the radiation source and when the analyte number densities both in the hot as well as in the cooler zones of the plasma are high.

Continuum radiation

Apart from the atom and ion lines of the species present in a plasma source, an emission spectrum has a continuum on which the emission lines are superimposed. This extends over the whole spectrum. It is due to the interactions between free electrons ("Bremsstrahlung") and to the interaction of free and bound electrons ("recombination continuum"). The former is particularly important in the UV spectral region, whereas the latter is important at longer wavelengths. The spectral intensity distribution for the continuum radiation is given by:

$$\begin{aligned} I(\nu) \cdot \mathrm{d}\nu = {} & K \times n_\mathrm{e} \times n_r \times r^2/(T_\mathrm{e})^{1/2} \times \exp[(-h\nu)/(kT_\mathrm{e})] \times \mathrm{d}\nu(\text{free–free}) \\ & + K' \times 1/(j^3) \times n_\mathrm{e} \times n_Z \times (Z^4)/(T_\mathrm{e}^{3/2}) \\ & \times \exp[-(U_j - h\nu)/kT_\mathrm{e}](\text{free–bound}) \end{aligned} \tag{57}$$

K and K' are constants, n_e is the electron number density, n_r is the number density of the ions with a charge of r times the elementary charge, T_e is the electron temperature, and is a measure of the kinetic energy of the electrons in the plasma. ν is the frequency, h and k are the Planck and Boltzmann constants, respectively, U_j is the ionization energy from the term with quantum number j, n_Z is the number density of the atoms with atomic number Z.

The intensity per unit of wavelength (radiant density B_λ) is obtained by multiplying with $4\pi c/\lambda^2$. Accordingly, for a hydrogen plasma the intensity of the "Bremsstrahlung" is given by:

$$B_\lambda = (2.04 \times 10^{-32} \times n_\mathrm{e}^2)/(\lambda^2 \times T_\mathrm{e}^{1/2}) \exp[-(1.44 \times 10^8)/(\lambda T_\mathrm{e})] \tag{58}$$

At complete ionization of the hydrogen (e.g. when added to a plasma with another gas as the main constituent) $n_\mathrm{e} = p/(2 \times k \times T_\mathrm{e})$ has a maximum at a wavelength of $\lambda = (7.2 \times 10^7)/T_\mathrm{e}$ or at a fixed wavelength, the maximum intensity is found at a temperature $T_\mathrm{e} = (5.76 \times 10^7)/\lambda$. Thus, the electron temperature can be determined from the wavelength dependence of the continuum intensity. As T_e is the electron temperature, absolute measurements of the background continuum emission in a plasma, e.g. for the case of hydrogen, allow determination of the electron temperature in a plasma, irrespective of whether it is in local thermal equilibrium or not. Similar methods also make use of the recombination continuum and of the ratio of the "Bremsstrahlung" and the recombination continuum.

1.4 Ionization

Provided that sufficient energy is transferred to a plasma, atoms can also be ionized. This depends on the temperature of the plasma and also on the ionization energy of the elements. As these ions have discrete energy levels between which

transitions are possible, just as atoms do, ionic spectra will also be important when considering the emission of radiation by a plasma. The ionization of atoms (a) of the element j into ions (i) is an equilibrium:

$$n_{aj} \leftrightharpoons n_{ij} + n_{\mathrm{e}} \tag{59}$$

and the equilibrium constant $S_{nj}(T)$, known as the Saha constant, is given by:

$$S_{nj}(T) = (n_{ij} \cdot n_{\mathrm{e}})/n_{aj} \tag{60}$$

The degree of ionization α_j for an element j is given by:

$$\alpha_j = n_{ij}/n_j = n_{ij}/(n_{aj} + n_{ij}) \tag{61}$$

n_{aj} and n_{ij} are the concentrations of the atoms and the ions and can be expressed as a function of the total number of atoms n_j by:

$$n_{aj} = (1 - \alpha_j) \cdot n_j \quad \text{and} \quad n_{ij} = \alpha_j \cdot n_j \tag{62}$$

Accordingly, using the notation given in Ref. [7], the intensity of an atom line can be written as:

$$I_{qp} = A_{qp} \cdot h \cdot \nu_{qp} \cdot g_q/Z_{aj} \cdot (1 - \alpha_j) \cdot n_j \cdot \exp(-E_q/kT) \tag{63}$$

and the intensity of an ion line is given by:

$$I^+_{qp} = A^+_{qp} \cdot h \cdot \nu^+_{qp} \cdot g^+_q/Z_{ij} \cdot \alpha_j \cdot n_j \cdot \exp(-E^+_q/kT) \tag{64}$$

These expressions for the intensities contain three factors that depend on the temperature, namely the degree of ionization, the Boltzmann factors, and the partition functions. In particular, α_j can be written as a function of the electron number density and the Saha function as:

$$[\alpha_j/(1 - \alpha_j)] \cdot n_{\mathrm{e}} = S_{nj}(T) \tag{65}$$

However, the latter is also given by the well-known Saha equation. With the aid of wave mechanics and through differentiation of the Boltzmann equation, the Saha function in terms of the partial pressures can also be expressed as:

$$\begin{aligned} S_{pj}(T) = (p_{ij} \cdot p_{\mathrm{e}})/(p_{aj}) &= [(2\pi m)^{3/2} \cdot (kT)^{5/2}]/h^3 \\ &\cdot 2Z_{ij}/Z_{aj} \cdot [\exp(-E_{ij}/kT)] \end{aligned} \tag{66}$$

The factor of 2 is the statistical weight of the free electron (2 spin orientations), $k = 1.38 \cdot 10^{-16}$ erg/K, $m = 9.11 \times 10^{-28}$ g, $h = 6.67 \times 10^{-27}$ erg s and 1 eV $= 1.6 \times 10^{-12}$ erg. This leads to the expression:

$$(P_{ij} \cdot p_e)/p_{aj} = S_{pj}(T) = 6.58 \times 10^{-7} \times T^{3/2} \times Z_{ij}/Z_{aj} \times [\exp_{10}(-5040 V_{ij}/T)] \quad (67)$$

or in the logarithmic form:

$$\log S_{pj} = 5/2 \log T - 5040/T \cdot V_{ij} + \log(Z_{ij})/(Z_{aj}) - 6.18 \quad (68)$$

where V_{ij} is the ionization energy (in eV).

The Saha equation is only valid for a plasma which is in local thermal equilibrium, where the temperature in the equation is then the ionization temperature. When this condition is not fulfilled, the equilibrium between the different states of ionization is given by the so-called Corona equation [16].

Accordingly, the degree of ionization in a plasma can be determined from the intensity relationship between an atom and an ion line of the same element as:

$$\log[(\alpha_j)/(1-\alpha_j)] = \log(I^+_{qp}/I_{qp}) - \log[(g^+_q \cdot A^+_{qp} \cdot v^+_{qp})/(g_q \cdot A_{qp} \cdot v_{qp})] + (5040/T)(V^+ - V_q) + \log(Z_{ij}/Z_{aj}) \quad (69)$$

This method can again only be applied for a plasma in local thermal equilibrium, the temperature of which is known. The partition functions Z_{aj} and Z_{ij} for the atom and ion species, respectively, are again a function of the temperature and the coefficients of these functions have been calculated for many elements [5]. Furthermore, the accuracy of the gA values and of the temperatures is important for the accuracy of the determination of the degree of ionization. One often uses the line pairs Mg II 279.6 nm/Mg I 278.0 nm and Mg II 279.6 nm/Mg I 285.2 nm for determinations of the degree of ionization of an element in a plasma.

Once α_j is known, the electron pressure can also be determined. Indeed, from

$$\log[\alpha_j/(1-\alpha_j)] = \log[S_{pj}(T)/p_e] \quad (70)$$

one can calculate

$$\log p_e = -\log[\alpha_j/(1-\alpha_j)] + \log S_{pj}(T) \quad (71)$$

When taking into account Eqs. (68) and (69), this results in:

$$\log p_e = -\log(I^+_{qp})/(I_{qp}) + \log(g^+_q \cdot A^+_{qp} \cdot v^+_{qp})/(g_q \cdot A_{qp} \cdot v_{qp}) - (5040/T)(V_{ij} + V^+_q - V_q) + 5/2(\log T) - 6.18 \quad (72)$$

By differentiating Eq. (72) with respect to temperature it can be found that the error in the determination of the electron pressure as a result of errors in the determination of the temperature is given by:

$$\mathrm{d}(\log p_e) = [(0.434 \times 5/2) + (5040/T)(V_{ij} + V^+_q - V_q)] \times (\mathrm{d}T/T) \quad (73)$$

Eq. (72) also shows that the intensity ratio of the atom and ion lines of an element will change considerably with the electron pressure in the plasma. Elements with a low ionization energy such as Na will thus have a strong influence on the intensity ratios of the atom and ion lines of other elements. This is analytically very important as it is the cause of the so-called ionization interferences found in classical DC arc emission spectrometry as well as in atomic absorption and plasma optical emission and in mass spectrometry.

When the plasma is not in local thermal equilibrium (LTE), the electron number densities cannot be determined on the basis of the Saha equation. Irrespective of the plasma being in local thermal equilibrium or not, the electron number density can be derived directly from the Stark broadening of the $H_ß$ line or of a suitable argon line. This contribution to broadening is a result of the electrical field of the quasi-static ions on one side and the mobile electrons on the other side. As described in Ref. [17], it can be written as:

$$\delta\lambda = 2[1 + 1.75\alpha(1 - 0.75\rho)]\omega \tag{74}$$

where ρ is the ratio of the distance between the ions (ρ_m) and the Debye path length (ρ_D), ω is the broadening due to the interaction of the electrons ($\approx n_e$) and α is the contribution of the interaction with the quasi-static ions ($\approx n_e^{1/4}$).

$$\rho_m = (4\pi \times n_e/3)^{-1/3} \tag{75}$$

$$\rho_D = [(k \times T)/(4\pi \times e^2 \times n_e)]^{1/2} \tag{76}$$

$\delta\lambda$ can thus be calculated as a function of n_e. Accordingly, from the widths of the Ar I 549.59 or the Ar I 565.07 nm lines, which are due mainly to Stark broadening, n_e can be determined directly and is independent of the existence of LTE. Thus, the temperature can also be determined when combined with measurement of the intensities of an atom line and an ion line of the same element. Indeed,

$$\log n_i/n_a = -\log n_e + 3/2 \log T - (5040/T) \cdot V_{ij} + \log(Z_{ij}/Z_{aj}) + 15.684 \tag{77}$$

which can be combined with Eq. (72).

Because with the "two-line method", using lines of the same ionization level for the determination of temperatures, it is difficult to fulfill all conditions necessary to obtain highly accurate values [see Eqs. (38) and (39)], a method was developed that enables the plasma temperature to be determined from intensities of lines belonging to different ionization levels. If I_i is the intensity of an ion line and I is the intensity of an atom line (in general both lines have to belong to two adjacent ionization levels), one can write:

$$\begin{aligned} I_i/I = {} & 2(A_i g_i \lambda_i / A g \lambda) \times [(2\pi m k T)^{3/2}/(h^3)] \times (1/n_e) \\ & \times (T^{3/2}) \times \exp[-(E_i - E + E_i - \Delta E_i)/(kT)] \end{aligned} \tag{78}$$

ΔE_i is a correction for the ionization energy of the lowest level. The plasma temperatures can also be determined from measurements of absolute line intensities. A survey of all methods used and discussed in the various chapters is given in Refs. [7, 8, 12].

Norm temperatures

From Eqs. (63) and (64), which give the intensity of a line, and from the Saha equation [Eq. (68)], it can be understood that for each spectral line emitted by a plasma source there is a temperature at which its emission intensity is maximal. This is the so-called norm temperature. In a first approximation [18], it can be written as:

$$T_n = (0.95 V_{ij} \times 10^3)/[1 - 0.33 \cdot \alpha + 0.37 \cdot \log(V_{ij}/10) - 0.14 \log P_e^*] \tag{79}$$

where V_{ij} is the ionization energy, $\alpha = V_a/V_{ij}$ and V_e is the excitation energy. P_e^* is the electron pressure (in atm; 1 atm $\approx$ 101 kPa) and is a function of T and n_e:

$$P_e^* = 1.263 \times 10^{-12} n_e \times T \tag{80}$$

In cases where we have to consider the norm temperature for a line of an element which is only present as an impurity in a plasma, e.g., one formed in a noble gas, the dilution in the plasma (a) also has to be considered. For a system with more components P_e^* is given by:

$$P_e^* = [(2i+1)/(2i+3)] \cdot (g_i/g_{i+1}) \cdot [4a/(1+a)^2] \cdot P \tag{81}$$

g_i and g_{i+1} are the statistical weights of the ions with charge i and $i+1$, respectively. Accordingly, as a result of the dilution, the change in the norm temperature (T_n) at a dilution of a will be given by:

$$\Delta T_n/T_n = 0.14 \log[4a/(1+a)^2] < 1 \tag{82}$$

At a dilution of 0.1 the change in norm temperature will thus be −7.2%. In a source such as the inductively coupled plasma the analyte dilution can be very high [of the order of 10^8 (1 mL/min of a 1–10 μg/mL solution for an element with a mass of 40, which is nebulized with an efficiency of 1% into an argon flow of 10 L/min). In an ICP the norm temperatures for lanthanum atom lines such as La I 418.7 nm ($V_{ij} = 5.61$ eV and $V_a = 2.96$ eV) will thus change from ca. 5000 K for a pure lanthanum plasma to 2830 K as a result of the large dilution. For atom lines of elements with relatively low ionization energies, the change in the norm temperatures as a result of the analyte dilution is high, but it is much less for ion lines. For the La II 412.3 nm line (second ionization energy: 11.43 eV and V_a: 3.82 eV) T_n is 9040 K.

From what is known about the norm temperatures, it becomes clear which types of lines will be optimally excited in a plasma of a given temperature, electron pres-

sure, and gas composition, and the norm temperatures thus give important indications for line selection in a source of a given temperature. Atom lines often have their norm temperatures below 4000 K, especially when the analyte dilution in the plasma is high, whereas those of ion lines often reach 10 000 K. The two types of lines are often denoted as ''soft'' and ''hard'' lines, respectively.

1.5 Dissociation

The dissociation of molecular plasma gases or analyte molecules which are brought into the radiation source is an equilibrium reaction. Accordingly, thermally stable radicals in particular or molecules are always present in a radiation source. They emit molecular bands which occur along with the atomic and ionic line spectra in the emission spectrum. Radicals and molecules may also give rise to the formation of cluster ions, the signals of which will be present in the mass spectra. The main species stemming from the plasma gases are: CN, NH, NO, OH, and N_2 (or N_2^+). From the analytes, predominantly thermally stable oxides remain (e.g., AlO^+, TiO^+, YO^+, etc.). A thorough treatment of molecular spectra is available in many classical textbooks (see, e.g., Refs. [19, 20]).

Molecules or radicals have different electronic energy levels ($^1\Sigma, {}^2\Sigma, {}^2\Pi, \ldots$), which have a vibrational fine structure ($v = 0, 1, 2, 3, \ldots$) and the latter again have a rotational hyperfine structure ($J = 0, 1, 2, 3, \ldots$). The total energy of a state is then given by:

$$E_\mathrm{i} = E_\mathrm{el} + E_\mathrm{vibr} + E_\mathrm{rot} \tag{83}$$

E_el is of the order of 1–10 eV, the energy difference between two vibrational levels of the same electronic state is of the order of 0.25 eV, and for the case of two rotational levels of a vibrational band the energy difference is of the order of only 0.005 eV. Through a transition between two rotational levels a rotational line is emitted. When the rotational levels considered belong to the same electronic level, the wavelength of the radiation emitted will be in the infrared region. When they belong to different electronic levels, the wavelength will be in the UV or in the visible region. Transitions are characterized by the three quantum numbers of the states involved, namely: n', v', j' and n'', v'', j''. All lines which originate from transitions between rotational levels belonging to different vibrational levels of two electronic states form the band: $n', v' \rightarrow n'', v''$. For these band spectra the selection rule is $\Delta j = j' - j'' = \pm 1, 0$. Transitions for which $j'' = j' + 1$ then give rise to the P-branch, $j'' = j' - 1$ to the R-branch, and $j' = j''$ to the Q-branch of the band. The line corresponding with $j' = j'' = 0$ is the zero line of the band. When $v' = v'' = 0$, it is also the zero line of the system. The difference between the wavenumber of a rotation line (in cm^{-1}) and the wavenumber of the zero line in the case of the P- and R-branches is a function of the rotational quantum number j and the rotational constant B_v for which:

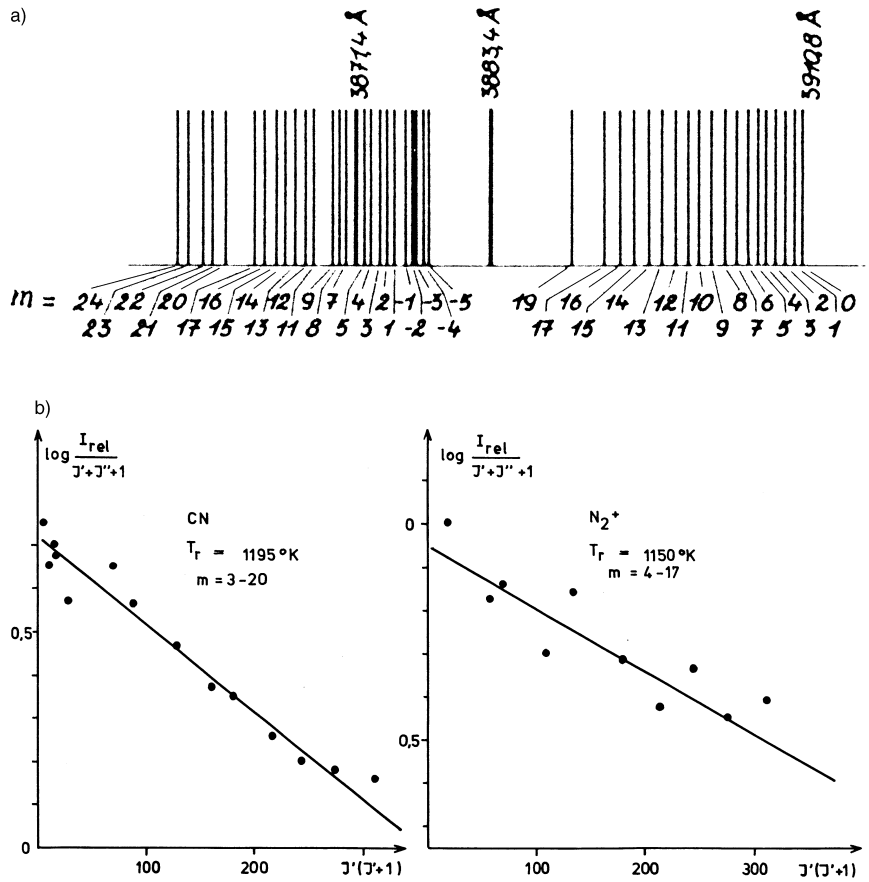

Fig. 3. Determination of rotational temperatures in a transitional hollow cathode. (a) Rotational lines used are of the R-branch of $^2\Sigma$–$^2\Sigma$ (0, 0) CN 388.3 nm and $^2\Sigma$–$^2\Sigma$ (0, 0) N_2^+ 391.4 nm band (positive $m = J'$ values belong to the R-branch); (b) Boltzmann plots for a graphite hollow cathode ($\phi_i = 4.76$ mm) operated at 80 mA and 330 Pa argon. (Reprinted with permission from Ref. [21].)

$$E_j/(hc) = B_v \cdot j(j+1) \tag{84}$$

The functional relationship is quadratic and is known as the Fortrat parabola.

For the CN radical and the N_2^+ molecular ion, the transitions giving rise to band emission between 370 and 400 nm, together with the rotational line pattern, are represented in Fig. 3 [21]. For the violet system of the CN band, there is no Q-branch and the lowest j in the R-branch is $j = 1$.

Molecular and radical band spectra thus consist of electronic series, which in turn consist of various vibrational bands, which again consist of rotational lines, many of which are often only partially resolved. As in the case of atomic spectral lines, the intensity of a rotational line can be written as:

$$I_{\mathrm{nm}} = N_{\mathrm{m}} \cdot A_{\mathrm{nm}} \cdot h \cdot \nu_{\mathrm{nm}} \cdot 1/2\pi \tag{85}$$

where N_{m} is the population of the excited level and ν_{nm} is the frequency of the emitted radiation. The transition probability for dipole radiation is:

$$A_{\mathrm{nm}} = (64 \cdot \pi^4 \cdot \nu_{\mathrm{nm}}^3)/3k \times 1/(g_{\mathrm{m}}) \times \Sigma|R_{n_i m_k}|^2 \tag{86}$$

i and k are degenerate levels of the upper (m) and the lower state (n). $R_{n_i m_k}$ is a matrix element of the electrical dipole moment and g_m is the statistical weight of the upper state. N_m is given by the Boltzmann equation:

$$N_m = N \cdot (g_m)/Z(T) \cdot \exp(-E_{\mathrm{r}}/kT) \tag{87}$$

where E_{r} is the rotational energy of the excited electronic and vibrational level and is given by:

$$E_{\mathrm{r}} = h \cdot c \cdot B_{v'} \cdot J' \cdot (J' + 1) \tag{88}$$

$B_{v'}$ is the rotational constant and J' is the rotational quantum number of the upper state (m). For a $^2\Sigma_{\mathrm{g}}$–$^2\Sigma_{\mathrm{u}}$ transition, the term $\Sigma|R_{n_i m_k}|^2 = J' + J'' + 1$, where J' and J'' are the rotational quantum numbers of the upper and the lower states, respectively. Accordingly:

$$\begin{aligned} I_{nm} = {} & (16 \cdot \pi^3 \cdot c \cdot N \cdot \nu_{nm}^4)/3Z(T) \cdot (J' + J'' + 1) \\ & \cdot \exp(-h \cdot c \cdot B_{v'} \cdot J'(J' + 1)/kT) \end{aligned} \tag{89}$$

or

$$\begin{aligned} \ln[I_{nm}/(J' + J'' + 1)] = {} & \ln[16 \cdot \pi^3 \cdot c \cdot N \cdot \nu_{nm}^4]/[3Z(T)] \\ & - [h \cdot c \cdot B_{v'} \cdot J'(J' + 1)]/kT \end{aligned} \tag{90}$$

By plotting $\ln[I_{nm}/(J' + J'' + 1)]$ versus $J'(J' + 1)$ for a series of rotational lines, a so-called rotational temperature can be determined. It characterizes the kinetic energy of the molecules and radicals responsible for emission of the band spectra. It is also a good approximation of the temperature, reflecting the kinetic energy of the neutrals and ions in a plasma. For the case of a hollow cathode discharge, the Boltzmann plot and the temperatures as measured from CN and N_2^+ band hyperfine structures are given in Fig. 3.

Spectral lines of molecular bands emitted by molecules and radicals present in a plasma often interfere with the atomic spectral lines in atomic emission spectrometry. However, in atomic absorption spectrometry the absorption by molecular bands stemming from undissociated molecules in the atom reservoir also leads to systematic errors and requires correction. Furthermore, in mass spectrometry molecular fragments give rise to signals, which can also interfere with the signals

from the ionized analyte atom. Therefore, it is important to study the dissociation of molecular species in the high-temperature sources used as radiation sources, atom reservoirs or ion sources. In different plasma sources a series of band-emitting species stem from the working gas. In this respect, for instance, N_2, N_2^+, CN, OH, and NH band emission has to be mentioned. However, undissociated sample and analyte species are also present in the plasma. In particular, thermally stable molecules such as AlO, LaO, BaO, AlF, CaF_2, and MgO may be present in atomic spectrometric sources. It is important to understand their dissociation as a function of the plasma temperature and the plasma composition. This dependence can be described by a dissociation equation, which is similar to the Saha equation:

$$K_n = [(2\pi/h^2) \cdot (M_X \cdot M_Y/M_{XY}) \cdot (kT)]^{3/2} \cdot (Z_X \cdot Z_Y/Z_{XY}) \cdot [\exp(-E_d/kT)] \quad (91)$$

where:

$$K_n = (n_X \cdot n_Y)/n_{XY} \quad (92)$$

Z represents the partition functions for the different atomic and molecular species, M_X, M_Y, and M_{XY} are the respective masses, and E_d is the dissociation energy.

This can be rewritten as:

$$\begin{aligned} \log K_n = {} & 20.432 + 3/2 \log(M_X \cdot M_Y/M_{XY}) + \log(Z_X \cdot Z_Y/Z_{XY}) \\ & - \log g + 1/2 \log T + \log B + \log(1 - 10^{-0.625\omega/T}) \\ & - (5040/T) \times V_d \end{aligned} \quad (93)$$

For most diatomic molecules B and ω (in cm^{-1}) have been listed in tables (see, e.g., Ref. [19]). V_d is then given in eV and for a diatomic molecule:

$$Z = [kT/(h \cdot c \cdot B)] \times [g \times \exp(-E_d/kT)]/[1 - \exp(h \cdot c \cdot \omega/kT)] \quad (94)$$

with $g = 1\ (^1\Sigma), 2\ (^2\Sigma, {}^1\pi, {}^2\pi_{1/2}, {}^2\pi_{3/2}, \ldots), 3\ (^3\Sigma, \ldots)$.

Thus, for a metal oxide (XY), from $n_{XY}/n_X = N_Y/K_n$ the ratio of the number densities for the metal oxide and the metal atoms (n_X) as well as the degree of dissociation can be calculated when the plasma temperature, the partial pressure of oxygen in the plasma (p_Y), and the dissociation constant are known. For refractory oxides of relevance in DC arc analysis, these data are listed, for example, in Ref. [7].

1.6 Sources for atomic spectrometry

In atomic spectrometry the sample material is brought into a high-temperature source (plasma, flame, etc.) with the aid of a sampling device. The sample, which

may be a liquid, a gas mixture or a solid, must be transformed into a vapor or an aerosol. This involves sample nebulization or various volatilization processes (e.g., by thermal evaporation or sputtering). It is advantageous to supply as much energy as possible for this process. The volatilization processes, the principle of which is to lead to a physical or chemical equilibrium, will possibly result in complete atomization, irrespective of the state of aggregation, of the eventual solid-state structure or of the chemical composition of the sample. This is very important both for obtaining the highest sensitivity as well as for keeping the matrix interferences involved in the analyses at the lowest possible level. The effectiveness of the volatilization processes involved, the plasma temperatures describing the kinetic energy distributions of the various plasma components as well as their number densities will all influence the atomization of the sample in the source.

The rotational temperatures are relevant to all processes in which molecules, radicals, and their dissociation products are involved. They can be obtained from the intensity distribution for the rotational lines in the rotation–vibration spectra, as described by Eqs. (83–90). The molecular fragments OH, CN, etc. have often been used to measure temperature (see, e.g., Refs. [21–23]).

The gas temperature is determined by the kinetic energy of the neutral atoms and the ions. It can be determined from the Doppler broadening of the spectral lines, as described by Eq. (49). However, to achieve this contributions of Doppler broadening and temperature broadening have to be separated, which involves the use of complicated deconvolution procedures as, e.g., shown for the case of glow discharges in Ref. [24].

Whereas the rotational temperature and the gas temperature are particularly relevant to the evaporation processes in the plasma, the electron temperature, being a measure of the kinetic energy of the electrons, is relevant to the study of excitation and ionization by collisions with electrons. This is an important process for the generation of the analyte signal both in optical atomic emission and in mass spectrometry. The electron temperature can be determined from the intensity of the recombination continuum or of the ''Bremsstrahlung'', as described by Eq. (57).

The excitation temperature describes the population of the excited levels of atoms and ions. Therefore, it is important in studies on the dependence of analyte line intensities on various plasma conditions in analytical emission spectrometry. It can be determined from the intensity ratio of two atomic emission lines of the same element and ionization state [see Eq. (40)] or from plots of the appropriate function for various atomic emission lines versus their excitation energies.

The ionization temperature is relevant for all phenomena involving equilibria between analyte atoms, ions, and free electrons in plasmas. In the case of thermal equilibrium, it occurs in the Saha equation [Eqs. (66, 68)] and can be determined from the intensity ratio of an ion line and an atom line of the same element. In all other cases, ionization temperatures can be determined from the n_e value obtained from Stark broadening [see Eqs. (74, 77)].

The different temperatures for the most important sources in atomic spectrometry are listed in Table 1.

In a plasma, which is at least in local thermal equilibrium, all the temperatures

Tab. 1. Temperatures (K) of sources used in atomic spectrometry.

Source	$T_{rotational}$	$T_{excitation}$	$T_{electron}$	$T_{ionization}$	
Arc discharges	5000	5000	5500	5000	LTE
Spark	–	20 000	20 000	20 000	LTE (transient)
Inductively coupled plasma	4800	5000	6000	6000	~LTE
Microwave plasmas	2000	4000	6000	6000	departures from LTE
Glow discharges	600	20 000	30 000	30 000	non-LTE

discussed are equal. In addition, this implies that the velocity distribution of all types of particles in the plasma (molecules, atoms, ions, and electrons) at any energy level can be described by the Maxwell equation [Eq. (17)]. For all species, the population of the different levels is then given by the Boltzmann equation [Eq. (19)]. Furthermore, the ionization of atoms, molecules, and radicals can be described by the Saha equation [Eqs. (66, 68)] and the related equations for the chemical equilibrium. Finally, the radiation density in the source conforms to Planck's law and the exchange of kinetic energy between the particles as well as the electromagnetic radiation exchange are in equilibrium with each other. The real plasma sources used in atomic spectrometry are at best in so-called local thermal equilibrium. However, contrary to the case of thermal equilibrium, all processes between the particles do not involve emission or absorption of electromagnetic radiation as the plasma cannot be considered as a completely closed system. Moreover, real plasma sources are extremely inhomogeneous with respect to temperature and species number density distributions. Accordingly, the above mentioned equilibria only occur within small volume elements of the sources, where gradients can be neglected.

Many plasmas, however, have a cylindrical symmetry and can be observed laterally. The observer then integrates the information provided for many volume elements along the observation direction and:

$$I(x) = 2\int_0^\infty I(x,y)\cdot \mathrm{d}y \tag{95}$$

where x and y are the coordinates of the volume element and integration of an intensity I is performed along the x-axis. When considering $I(r)$, with r the radial distance away from the plasma center (Fig. 4), this becomes:

$$I(x) = 2\int_x^\infty I(r)\cdot r\cdot \mathrm{d}r/[\sqrt{(r^2-x^2)}] \tag{96}$$

From these integral values, the values at a well-defined radial distance away from the plasma center can be calculated. This necessitates side-on observation along several parallel axes, which are equidistant with respect to each other, and an Abel inversion. Indeed, if $I'(x)$ is the first derivative of the function $I(x)$, describing the

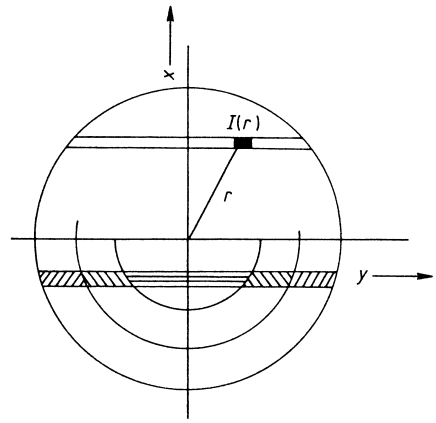

Fig. 4. Abel inversion procedure used for the determination of radial distributions in plasma sources. x: lateral position, y: direction of observation, r: radial distance.

variation of a measured value as a function of the lateral position (x) during side-on observation (Fig. 4), the radial values at a distance r are given by:

$$I(r) = -(1/\pi)\int_r^{\infty} [I'(x) \cdot \mathrm{d}x]/\sqrt{(r^2 - x^2)} \tag{97}$$

This integral can only be solved numerically. One has to write each laterally measured intensity as a sum of the different volume elements with a given coefficient denoting their contribution. For certain numbers of lateral observation positions $(3, 10, \ldots)$ these Abel coefficients are listed in the literature [25]. By inversion of the corresponding matrix the radial values are then obtained. This allows determination of the radial distributions of emissivities, absorbances, temperatures or species number densities in plasmas. By repeating this procedure at different heights in a plasma one can perform plasma tomography. Similar results, which do not require the assumption of cylindrical symmetry in the source, can now be obtained by imaging spectrometry using two-dimensional detectors (for a discussion, see, e.g., Ref. [26]).

In real plasmas, departures from thermal equilibrium often occur. For the extreme case, as encountered in plasmas under reduced pressure, the emission or the absorption of radiation becomes so important that there is no longer a clear relationship between the mean kinetic energies of the species and the excitation temperatures. The latter then lose the physical meaning of a temperature. The absence of local thermal equilibrium in these so-called non-LTE plasmas relates to the existence of high field gradients or AC fields, by which only the light electrons and not the heavy atoms and ions can follow the field changes and take up the dissipated energies fully. Accordingly, the mean kinetic energy of the electrons and thus also the electron temperature will be much higher than the gas kinetic temperature. For a plasma that is not in local thermal equilibrium, the equilibrium between species at different ionization levels at different temperatures will be given by the

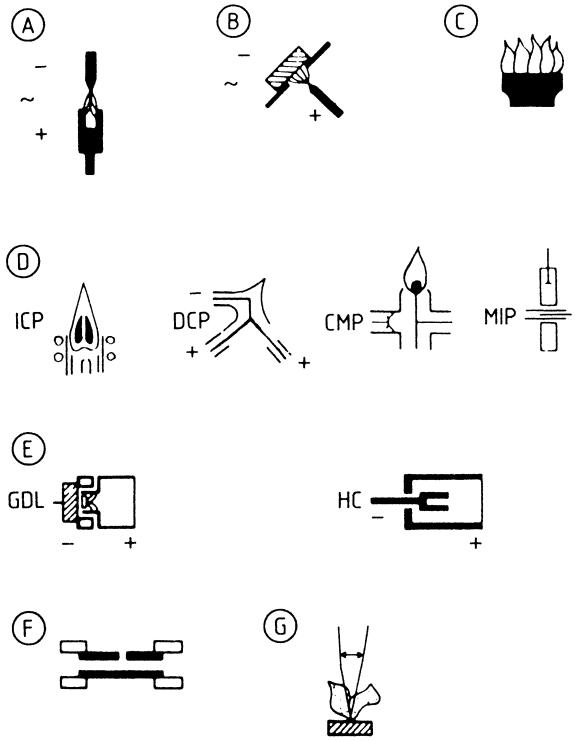

Fig. 5. Sources for atomic spectrometry (Reprinted with permission from Ref. [28].) (A): arc; (B): spark; (C): flame; (D): plasma sources; (E): low-pressure discharges; (F): furnace; (G): laser.

so-called Corona equation, as is, for example, derived for the sun by astrophysicists [27].

Sources for atomic spectrometry include flames, arcs, sparks, low-pressure discharges, and lasers, as well as DC, high-frequency, and microwave plasma discharges at reduced and atmospheric pressures (Fig. 5) [28]. They can be characterized as listed in Table 2. Flames are in thermal equilibrium. Their temperatures, however, are at the highest only 2800 K. As this is far below the norm temperature of most elemental lines, flames are only of limited importance for atomic emission spectrometry, but they are excellent atom reservoirs for atomic absorption and atomic fluorescence spectrometry as well as for laser-enhanced ionization work. Arcs and sparks are well known as sources for atomic emission spectrometry. In view of the high temperatures obtained in spark sources, it can be anticipated that ion lines in particular will be excited, the norm temperatures of which are often beyond 10 000 K, whereas in arc sources atom lines will be predominant. In plasma sources under reduced pressure the gas kinetic temperatures are low. Accordingly, their atomization capacity will be limited. When these sources are used as both atomic emission sources and as primary sources in atomic absorption the line widths will be very narrow. Moreover, particularly when gases with high ionization energies such as helium are used, lines with high excitation energies, such as those of the halogens, can also be excited. Discharges under reduced pres-

Tab. 2. Use of sources in analytical atomic spectrometry.

Source	*Optical spectrometry*			*Mass spectrometry*
	emission	*absorption*	*fluorescence*	
Chemical flame	+	+	+	
Arc	+			+
Spark	+			+
Electrically-heated furnace	+	+	+	+
Arc jet plasma	+			
Inductively coupled plasma	+		+	+
Microwave plasma	+	+		+
Glow discharge	+	+	+	+
Laser plasma	+	+	+	+
Exploding wire/foil	+			

sure are valuable ion sources for mass spectrometry as analyte ionization takes place, and because of the low pressure the coupling with a mass spectrometer operated at 10^{-5} mbar becomes easier. So-called plasma jet and plasma sources at atmospheric pressure are of particular use for the emission spectrometric analysis of solutions. Their gas kinetic temperatures are high enough so as to achieve a complete dissociation of thermally stable oxides and both atom lines as well as ion lines occur in the spectra. As reflected by the fairly high ionization temperatures, they are powerful ion sources for mass spectrometry, and plasma mass spectrometry is now one of the most sensitive methods of atomic spectrometry. Lasers are very suitable devices for material ablation in the case of solids. Owing to their high analyte number densities, plasmas are subject to high self-absorption and thus it is more appropriate to use them only as sources for material volatilization and to lead the ablated material into a second source.

1.7 Analytical atomic spectrometry

Analytical atomic spectrometry nowadays includes the use of flames and plasma discharges for optical and mass spectrometry. The sources are used directly as emission sources or atom reservoirs for atomic absorption or atomic fluorescence or they are used for ion production. In optical atomic spectrometry, atomic emission, absorption, and fluorescence all have their specific possibilities and analytical features. The type of information obtained is clear from the transitions involved (Fig. 6).

In atomic emission, thermal or electrical energy is used to bring the analyte species to an excited state, from which they return to their ground state through emission of radiation characteristic of all the species present that were sufficiently excited. Thus, from the principle of atomic emission spectrometry it is clearly a

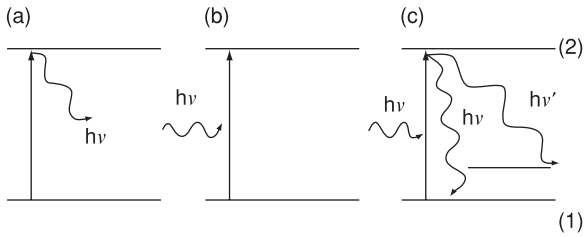

Fig. 6. Term schemes for (a): atomic emission, (b): absorption, and (c): fluorescence spectrometry (resonant: $h\nu$ and non-resonant: $h\nu'$).

multielement method. The number of elements that can be determined simultaneously is only limited by the availability of sufficiently sensitive interference-free spectral lines. In the case of atomic emission spectrometry, the selectivity is achieved by the isolation of the spectral lines with the aid of the exit slit of the spectrometer. This puts high demands on the optical quality of the spectral apparatus used and certainly requires a spectrometer with high spectral resolution. Moreover, the lines are superimposed on a spectral background, which is partly structured as the result of the presence of radicals and molecular ions emitting band spectra. Broad wings arising from neighboring spectral lines, e.g. of matrix constituents, may also occur and finally there will be a continuum resulting from the interaction of free and bound electrons (see Section 1.3, continuum radiation). The intensity of the spectral background on which the line to be measured is superimposed, may thus differ considerably from one sample to another. It must be subtracted from the total line intensities, as only the radiation emitted by the analyte atoms is relevant for the calibration. This can be done by estimating the spectral background intensity "under" the analytical line for the background intensities at the wavelength of the analytical line using a blank sample. It is often safer to estimate it from the spectral background intensities close to the analytical line (e.g. on each side) in the spectrum of the sample itself. The latter is certainly the case when the line is positioned on a wing of a band or a broad matrix spectral line, providing different spectral background intensities on either side of the analytical line. The means to correct for the spectral background must be available in every atomic emission spectrometer used for trace analysis.

In atomic absorption spectrometry we need a primary source delivering monochromatic radiation of which the wavelength matches that of a resonance line of the element to be determined. The spectral width must be narrow with respect to the absorption profile of the analyte line. From this point of view, atomic absorption is a single-elemental method, of which the dynamic range is usually much lower than in atomic emission spectrometry. It is, to a first approximation, a zero-background method, when neglecting absorption due to radiation scattering and molecular absorption. As the final spectral selectivity is realized by the primary source, the spectral apparatus only has to enable line isolation in a spectrum of the element to be determined, where the spectral lines are very narrow. Accordingly, the demands on the spectral resolving power of the spectrometer are much lower than in atomic emission spectrometry.

In atomic fluorescence, the excitation can be performed both with white as well as with monochromatic sources, which consequently affects the fluorescence intensities obtainable and the freedom from stray radiation limitations. The latter are particularly low with monochromatic primary sources and when using fluorescence lines with wavelengths differing from that of the exciting radiation. Generally, in atomic fluorescence the linear dynamic range is higher than in atomic absorption and spectral interference as well as background interferences are just as low.

In the case of atomic absorption and atomic fluorescence the selectivity is thus already partly realized by the radiation source delivering the primary radiation, which in most cases is a line source (hollow cathode lamp, laser, etc.). Therefore, the spectral bandpass of the monochromator is not as critical as it is in atomic emission work. This is especially true for laser-based methods, where in some cases of atomic fluorescence a filter is sufficient, or for laser-induced ionization spectrometry where no spectral isolation is required at all.

For glow discharges and inductively coupled high-frequency plasmas, ion generation takes place in the plasmas. In the first case, mass spectrometry can be performed directly on solids and in the second case on liquids or solids after sample dissolution. In the various atomic spectrometric methods, real samples have to be delivered in the appropriate form to the plasma source. Therefore, in the treatment of the respective methods extensive attention will be given to the techniques for sample introduction.

In an atomic spectrometric source, both the atomic vapor production as well as signal generation processes take place. The first processes require high energy so as to achieve complete atomization as already discussed, whereas the signal generation processes in many cases would profit from a discrete excitation which makes use, for example, of the selective excitation of the terms involved. Therefore, in a number of cases, the use of so-called tandem sources, where the analyte vapor generation and the signal generation take place in a different source (for a discussion, see Ref. [29]), may offer advantages with respect to the power of detection as well as freedom from interferences.